Predictive model for the intra-diffusion coefficients of H_2 and O_2 in vapour H_2O based on data from molecular dynamics simulations

Othonas A. Moultos & Ioannis N. Tsimpanogiannis

Published online: 15 May 2023.

Submit your article to this journal

Article views: 88

View related articles

View Crossmark data

Taylor & Francis
Taylor & Francis Group

THERMODYNAMICS 2022 SPECIAL ISSUE (BY INVITATION ONLY)

Check for updates

Predictive model for the intra-diffusion coefficients of H_2 and O_2 in vapour H_2O based on data from molecular dynamics simulations

Othonas A. Moultos [ID][a] and Ioannis N. Tsimpanogiannis [ID][b]

[a]Engineering Thermodynamics, Process & Energy Department, Faculty of Mechanical, Maritime and Materials Engineering, Delft University of Technology, Delft, The Netherlands; [b]Chemical Process & Energy Resources Institute (CPERI), Centre for Research & Technology Hellas (CERTH), Thermi-Thessaloniki, Greece

ABSTRACT
Available data from experiments and molecular simulations for the intra-diffusivities of H_2 and O_2 in H_2O, and for the self-diffusivity of pure H_2O (at pressure and temperature conditions in which the solvent is in the vapour phase) are compared against calculations based on the Chapman-Enskog theory or other semi-empirical/semi-theoretical methods. A novel methodology is proposed to extrapolate the intra-/self-diffusivities data computed from molecular dynamics simulations at low pressures. The extrapolated values are used to further refine the recently-proposed [Tsimpanogiannis et al., J. Chem. Eng. Data, 66, 3226-3244, (2021)], molecular simulation based correlation of intra-/self-diffusivities as a function of pressure and temperature with the solvent being in the vapour phase.
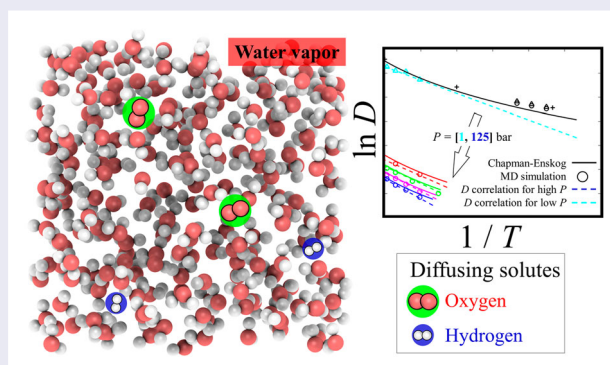
1. Introduction

Understanding the mass transport of H_2 and O_2 in aqueous solutions is crucial for the optimal design of systems such as fuel cells [1] and water electrolysers [2], and for controlling processes such as the air-water gas exchange [3]. Also the mutual diffusion of H_2 and H_2O in vapour or liquid phases is encountered during the large scale H_2 storage in geological formations [4–6]. The storage of H_2 is a major issue that needs to be solved in an adequate matter in order to advance from the current 'Carbon-based Economy' towards a 'H_2-based Economy' [7,8]. As it was discussed in detail in previous studies

[9–11], the intra-diffusivities can be obtained via experimental measurements, semi-theoretical/semi-empirical models, and molecular simulations. A limitation of measuring intra-diffusivities experimentally is that in, most cases, the experiments can be performed at/or close to the atmospheric pressure [12]. Thus, experimental diffusivity data for higher pressures (and very often, temperatures) are relatively scarce. One of the approaches considered for overcoming this lack of data is through the use of semi-empirical approaches [13–15]. Such approaches can be further guided by theory, i.e. the Chapman-Enskog [16] theory for the case of diffusion in

vapour/gaseous phase, or the Stokes-Einstein [14,17] theory for the case of diffusion in liquid phase. Although the semi-empirical methods are relatively easy to use and computationally fast, their accuracy depends on the extent and quality of the experimental data that was used for their development (i.e. calibration step). Therefore, the accuracy of the data is an important factor that can improve the quality of the predictions of semi-empirical methods. Furthermore, semi-empirical methods provide very limited insight into the transport mechanisms occurring in the real system. In sharp contrast, Molecular Dynamics (MD) simulations are able to provide detailed physical insight, since MD accesses atomistic length- and time-scales. MD is significantly more computationally demanding [18,19] than semi-empirical methods, while requires an accurate description of the intra- and inter-molecular interactions, which are implemented in the form of parameterised potential functions, known as force fields. In the past few decades, with the significant rise of computational power, the development of efficient open-source MD software, and the parameterisation of accurate force fields for many chemical components, MD simulations have been evolved to a reliable and widely used tool for computing diffusivities (and many other transport and thermodynamic properties) of pure components and mixtures [10,20–33]. Often, the data (e.g. diffusivities of gases in H_2O) produced with MD simulations are further used for the development of engineering models and the validation of semi-empirical approaches [10].

Although, the intra-diffusivities of H_2 and O_2 in liquid H_2O have been recently studied, the respective diffusivities in the gas phase, especially at low pressures, have not attracted much attention. For this reason, the purpose of this study is (a) to utilise the recent wide collection of MD data [10] for the intra-diffusivities of H_2 and O_2 in vapour H_2O and compare them with values obtained from the Chapman-Enskog theory and other semi-theoretical/semi-empirical models, (b) to evaluate the MD data by comparing with the available experimental data, and (c) to develop a novel methodology able to extrapolate the intra-diffusivities computed in MD to lower pressures. It is important to note that in the H_2/H_2O and O_2/H_2O systems considered here, the gases are in the infinite dilution limit. Thus, there is no need to consider the effect of gas composition in the development of the new methodology. For systems with higher solute concentrations, the composition of the mixture may be an important parameter in a predictive model for intra-diffusivities. Moreover, for such systems, the prediction of mutual diffusivities (i.e. Maxwell-Stefan, Fickian) is also of interest since these diffusivities strongly depend on the composition of the mixture [13,26]. On the contrary, for the systems considered here, the intra-, Maxwell-Stefan, and Fickian diffusivity are by definition equal [13,26]. The remainder of this manuscript is organised as follows: In Section 2, we describe the theoretical background and the methodology followed for the computing the intra-diffusivities of H_2 and O_2 in vapour H_2O. In Section 3, we present and discuss in detail, the comparison between the intra-diffusivities computed in MD and those obtained from using the Chapman-Enskog theory, the semi-empirical models, and the available experimental values. We also describe the development of a novel methodology to extrapolate the MD data to lower pressures. Finally, in Section 4, the conclusions and a future outlook are presented.

2. Methodology

2.1. Chapman-Enskog theory

Chapman and Enskog [14,16], working independently, developed a theory resulting from the solution of the Boltzmann equation, that describes the diffusion in binary gas mixtures (D_{AB}) at low to moderate pressures [14,34]. The equation describing the theory is as follows:

$$D_{AB} = \frac{3}{16} \frac{(4\pi kT/M_{AB})^{1/2}}{n\pi \sigma_{AB}^2 \Omega_D} f_D \tag{1}$$

where k is the Boltzmann constant, T is the temperature of the system, $M_{AB} = 2[(1/M_A) + (1/M_B)]^{-1}$ (where M_A and M_B are the molecular weights of components A and B, respectively), n is the number density of the molecules in the mixture, $\sigma_{AB} = \frac{\sigma_A + \sigma_B}{2}$ is a characteristic length of the intermolecular force field, Ω_D is the collision integral for diffusion, and f_D is a correction term which is of the order of unity. If we assume $f_D = 1.0$ and that n follows from the ideal-gas law, Equation (1) reduces to:

$$D_{AB} = \frac{0.00266 T^{3/2}}{P M_{AB}^{1/2} \sigma_{AB}^2 \Omega_D} \tag{2}$$

where D_{AB} is in units of cm²/s, T in K, pressure (P) in bar, and σ_{AB} in Å. Ω_D is dimensionless.

Values for Ω_D have been tabulated for the 12-6 Lennard-Jones (LJ) potential (see Hirschfelder et al. [35]) as a function of kT/ϵ, where ϵ is the LJ energy parameter. Here, we use the accurate analytical approximation reported by Neufeld et al. [36]:

$$\Omega_D = \frac{A}{(T^*)^B} + \frac{C}{\exp(DT^*)} + \frac{E}{\exp(FT^*)} + \frac{G}{\exp(HT^*)} \tag{3}$$

where $T^* = kT/\epsilon_{AB}$, $\epsilon_{AB} = (\epsilon_A\epsilon_B)^{1/2}$, $A = 1.06036$, $B = 0.15610$, $C = 0.19300$, $D = 0.47635$, $E = 1.03587$, $F = 1.52996$, $G = 1.76474$, and $H = 3.89411$.

It should be pointed out that Equation (2) has been developed for the diffusion in dilute gases consisting of spherical, monoatomic, nonpolar molecules. When coupled with the Lennard-Jones potential it can produce reasonable results for a wide range of temperatures (Poling et al. [14]). A detailed review on the theoretical basis and experimental-related issues for the diffusivity in the gas/vapour phase has been provided by Marrero and Mason [37]. However, if the components are polar it is essential to use a more refined potential (e.g. Stockmayer), resulting in a different type of collision integral. In order to account for polarity during the calculation of diffusivities, Brokaw [34] recommended the use of Equation (1), coupled with the following equation for the collision integral

$$\Omega_D = \Omega_D[\text{Equation (3)}] + \frac{0.19\delta_{AB}^2}{T^*} \qquad (4)$$

with δ_{AB} given by the following combining rule: $\delta_{AB} = (\delta_A\delta_B)^{1/2}$, while δ_A or δ_B for the pure components (A or B) are calculated from the following equation:

$$\delta_i = \frac{1.94 \times 10^3 \mu_p^2}{V_b T_b} \qquad (5)$$

where i denotes the pure component (A or B), μ_p is the dipole moment (in [debyes]), V_b is the liquid molar volume (in [cm^3/mol]) at the normal boiling point (1 atm), and T_b is the normal boiling point (in [K]) of the pure components.

2.2. Semi-theoretical/semi-empirical methods

Poling et al. [14] provided a detailed list of studies exploring semi-empirical methods for the calculation of the diffusivities in the vapour phase at low pressures. In this study, we focus on two such methods, i.e. the Wilke and Lee [38]

$$D_{AB} = \frac{[3.03 - (0.98/M_{AB}^{1/2})]10^{-3}T^{3/2}}{PM_{AB}^{1/2}\sigma_{AB}^2\Omega_D} \qquad (6)$$

and the Fuller et al. [39–41]

$$D_{AB} = \frac{0.00143T^{1.75}}{PM_{AB}^{1/2}[(\sum_u)_A^{1/3} + (\sum_u)_B^{1/3}]^2} \qquad (7)$$

In Equation (6) and (7), D_{AB} is in cm^2/s, T in K, P in bar, σ_{AB} in Å, and M_A and M_B in g/mol. $\sum_u$ indicated the summation of the atomic diffusion volumes (i.e. 6.12 for H$_2$, 16.3 for O$_2$, and 13.1 for H$_2$O) [40].

2.3. MD simulation data

Recently, Tsimpanogiannis et al. [10] performed extensive MD simulations to compute the intra-diffusivities of H$_2$ and O$_2$ in H$_2$O, at the limit of infinite dilution for a wide temperature and pressure range. The authors evaluated the performance of six H$_2$ and six O$_2$ force fields combined with the TIP4P/2005 H$_2$O force field [42] in predicting the density, self-diffusion coefficients, and viscosities of the pure gases, and the self-diffusion coefficients of the gases in H$_2$O at low pressures. Tsimpanogiannis et al. [10] concluded that the following force field combinations were the most accurate; the Buch [43] – TIP4P/2005 for the intra-diffusivities of H$_2$ in H$_2$O, and the Bohn [44] – TIP4P/2005 for the corresponding case of O$_2$. These force fields were used to compute the intra-diffusion coefficients of H$_2$ and O$_2$ in H$_2$O for a wide temperature (275.15–975.15 K) and pressure (0.1–200 MPa) range that span the vapour, liquid, and supercritical conditions. It is important to note that the data-set reported by Tsimpanogiannis et al. [10] contains diffusivities corrected for finite size effects [45–49], and with relatively low uncertainties (max. 10%). The authors correlated the MD data to develop engineering models for predicting the self-diffusivities of pure H$_2$O and the intra-diffusivities of H$_2$ and O$_2$ in H$_2$O. The model for the diffusion in the vapour phase is as follows:

$$D = \exp\left[(n_1P + n_0) + (m_1P + m_0)\frac{1}{T}\right] \qquad (8)$$

where D is the self- or intra-diffusivity, and m_o, m_1, n_o, and n_1 are fitting parameters. The calculated fitting parameters for the three systems considered here (self-diffusivities of pure vapour H$_2$O and the intra-diffusivities of H$_2$ and O$_2$ in vapour H$_2$O) are listed in Table 1 and in the original work [10].

2.4. Data from experimental studies

Marrero and Mason [37] presented a detailed review on the theoretically predicted and experimentally measured diffusivities in the gas/vapour phase. An updated review has also been provided by Poling et al. [14]. Here, the following sources of experimental data have been used:

Case 1. H$_2$ in H$_2$O: Nelson [50] reported three experimental measurements for the diffusivity of water vapour in H$_2$ at a pressure of 760 mm Hg and temperatures in the range 298–328 K. Crider [51] reported two experimental measurements for the diffusivity of water vapour in H$_2$ at a pressure of 760 mm Hg and temperatures in the range 307–329 K. Schwertz and Brow[52] reported three experimental measurements for the mutual coefficients of diffusion for the system H$_2$ – H$_2$O at a pressure of

Table 1. Parameters of the generalised Equation (8) for predicting the intra-diffusivities of infinitely diluted H_2 and O_2 in vapour H_2O, and the self-diffusivity of pure vapour H_2O (Tsimpanogiannis et al. [10]).

	H_2 in H_2O	O_2 in H_2O	pure H_2O
m_0	$(-1.21 \pm 0.06) \times 10^3$	$(-1.10 \pm 0.06) \times 10^3$	$(-1.45 \pm 0.09) \times 10^3$
m_1	$(-0.39 \pm 0.07) \times 10^1$	$(-0.43 \pm 0.07) \times 10^1$	$(-0.61 \pm 0.09) \times 10^1$
n_0	-9.35 ± 0.12	-10.98 ± 0.04	-10.63 ± 0.01
n_1	$(-0.92 \pm 0.13) \times 10^{-2}$	$(-0.63 \pm 0.05) \times 10^{-2}$	$(-0.40 \pm 0.01) \times 10^{-2}$

760 mm Hg and temperatures in the range 307–353 K. McMurtie and Keyes [53], reported a series of experimental measurements for four temperatures in the range 303–333 K, at low pressures.

Case 2. O_2 in H_2O: Walker and Westenberg [54] reported seven experimental measurements for the mutual coefficients of diffusion for the system O_2 – H_2O at a pressure of 1 atm and temperatures in the range 300–300 K. The authors also reported three extrapolated/correlated values in the range 308–352 K to compare with specific literature values. Both measured and extrapolated values are used in the comparisons reported in this study. Schwertz and Brow [52] reported three experimental measurements for the mutual coefficients of diffusion for the system H_2 – H_2O at a pressure of 760 mm Hg and temperatures in the range 308–352 K.

Case 3. pure H_2O: Matsunaga and Nagashima [55] reported experimental measurements for the self-diffusion coefficients of H_2O at 0.1 MPa and temperatures in the range 273–2000 K.

3. Results and discussion

### 3.1. Comparison with the chapman-Enskog theory and two semi-theoretical/semi-empirical methods

Figure 1(a,b) show Arrhenius plots for the cases of H_2 and O_2 intra-diffusion in vapour H_2O, respectively, at $P = 50$, 75, 100, and 125 bar. Each one of the sub-figures shown in Figure 1 includes: (i) MD simulations (symbols), (ii) the calculations using the Chapman-Enskog (CE) theory (solid lines), (iii) the calculations using the recommended correlations by Tsimpanogiannis et al. [10] (dashed lines), and (iv) the calculated values using the semi-empirical methods of Wilke and Lee [38] (dashed-dotted lines), and Fuller et al. [40] (dotted lines). As can be seen, for constant pressure, the agreement between the MD data and the CE calculations improve as the temperature increases (i.e. moving away from the critical point). The MD simulations exhibit a dependency on T of the following type: $\ln D \propto (1/T)$. The data produced with CE theory have a more complex dependency, i.e. $\ln D \propto (\frac{T^{3/2}}{\Omega_D})$. Close to the critical point, the diffusivities computed in MD simulations and those obtained

from theoretical calculations start to deviate significantly. To clarify the origins of this discrepancy, more MD simulations need to be carried out in close proximity to the critical point.

Similarly, Figure 1(c) shows the corresponding Arrhenius plot for H_2O self-diffusivity. In this calculation, the polarity of water is taken into account via Equation (4). Figure 1(d) shows the corresponding Arrhenius plot for H_2O self-diffusivity ignoring the water polarity. Namely, using Equation (3) for the calculation of the collision integrals. When the polarity is ignored, the calculated values for the diffusivity further deviate (overprediction) from the MD simulations by approximately 5–8 %. This becomes clear in Figure 2 where the percentage deviation ($\%dev. = 100 \times \frac{D_\text{polar} - D_\text{no-polar}}{D_\text{polar}}$) between the calculations with (D_polar) and without polarity ($D_\text{no-polar}$) considered is shown as a function of the inverse T. Water has a dipole moment, $\mu_p = 1.8$ debyes [14], therefore the contribution of the term for polarity correction, $\frac{0.19\delta_{AB}^2}{T^*}$, in Equation (4) is responsible for the reduction by approximately 5–8 % that results when taking into account polarity effects through Equation (4). It should also be noted that H_2 and O_2 have a dipole moment equal to zero. Interestingly, at constant T, all data are independent of pressure. Such behaviour should be expected since the correction term in Equation (4), which accounts for the polarity correction, does not depend on pressure. Finally, regarding the comparison with the semi-empirical methods of Wilke and Lee [38], and Fuller et al. [40] we observe the following: For the cases of (i) H_2 intra-diffusion in vapour H_2O, and (ii) H_2O self-diffusivity, the Wilke and Lee method results in diffusivity predictions that are very close to those calculated with the CE theory. In particular, the Wilke and Lee method results in a slight under-prediction of diffusivity for the case of H_2, while it slightly over-predicts diffusivity for the case of H_2O self-diffusivity. On the other hand, for both the aforementioned cases, the Fuller et al. method results in diffusivity over-predictions by about 7–10 %. For the case O_2 intra-diffusion in vapour H_2O, both the Wilke and Lee and the Fuller et al. methods are in very good agreement between themselves, as well as, with the CE theory. Both methods slightly over-predict the diffusivity values.
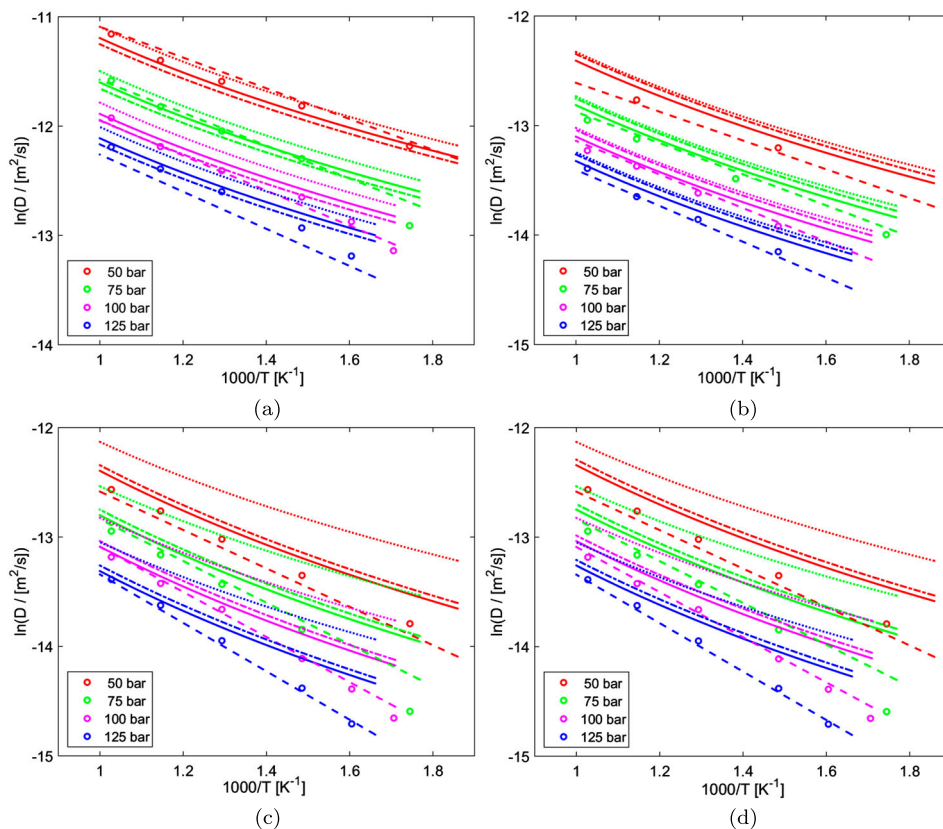
Figure 1. Arrhenius-type plots of the computed/calculated intra-diffusion coefficients of H_2 in H_2O (a), O_2 in H_2O (b), pure H_2O accounting for water polarity (c), and pure H_2O without accounting for water polarity (d), occurring in the vapour phase. Circles denote the MD simulations reported by Tsimpanogiannis et al. [10]. Dashed lines denote calculations with the correlation [Equation (8)]. Solid lines denote calculations with the CE theory. Dashed-dotted lines denote calculations with the Wilke and Lee [38] method, while dotted lines denote calculations with the Fuller et al. [40] method. Lines and symbols of the same colour correspond to a particular pressure.
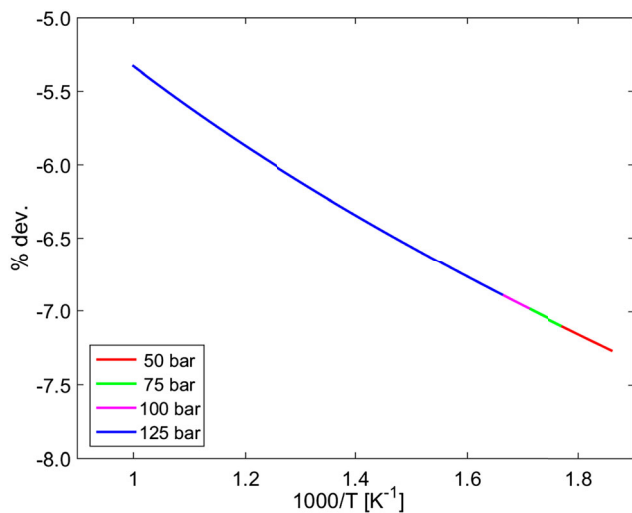
Figure 2. Percentage deviation (%*dev.*) between the calculations of the self-diffusivity accounting for polar contributions (D_{polar}) and without accounting for polarity ($D_{no-polar}$), shown as a function of the inverse T for the case of pure H_2O self-diffusion.

3.2. Comparison with experimental studies

To the best of our knowledge, the only available experimental studies for the three systems of interest (i.e. H_2 or O_2 diffusing in vapour H_2O, and H_2O self-diffusion in the vapour phase) are at low P (i.e. 1 atm). Figure 3(a–c) show the comparison of the available experimental data with the calculations from the CE theory, and the two semi-empirical methods (Wilke and Lee [38] and Fuller et al. [40]) for H_2 and O_2 intra-diffusion in vapour H_2O, and H_2O self-diffusion, respectively. For all systems, we observe that the CE theory and the Wilke and Lee method result in almost identical predictions, while the method of Fuller et al. over-predicts the diffusivities, with the case of the self-diffusivity of pure H_2O vapour being the least accurate. For the case of H_2 intra-diffusivity in vapour H_2O, we further observe (Figure 3(a)) that all the available experimental data fall between the calculations from the CE theory and the Fuller et al. method. For O_2 intra-diffusivities in vapour H_2O (Figure 3(b)), it is clear

that the experimental data are very well capture by the method of Fuller et al., while the calculations with the CE theory and the Wilke and Lee method produce under-predictions. Finally, the experimental measurements of the self-diffusivity of vapour H_2O (Figure 3(c)) are very well described by the calculations from the CE theory and the Wilke and Lee method, while the calculations with the Fuller et al. method yield an over-predictions of 6–10 %.

In the recent study of Tsimpanogiannis et al. [10], MD simulations of H_2O in the vapour phase, have been reported only for P=50, 75, 100, and 120 bar. As the pressure decreases, the volume of the system (and thus, the simulation box and the empty space within) increases significantly, making MD simulations very inefficient. This practically means, that for gas systems, MD simulations become prohibitively slow. Therefore, the only possible comparison with the MD simulations can be made by using Equation (8) and extrapolating the diffusivity computations to the low pressures of interest (i.e. 1

atm). These extrapolations are shown in Figure 3 as black dashed lines. While Equation (8) can accurately describe the MD simulations within the range of development (i.e. 50–125 bar), the extrapolation to lower pressures is rather poor. To rectify this issue, we devised a novel methodology which is described in the following section.

### 3.3. Methodology development

Figure 4(a–c) show the H_2 and O_2 intra-diffusion coefficients in vapour H_2O, and H_2O self-diffusion, respectively, computed with MD simulations as a function of the inverse pressure $(1/P)$ at $T = 673, 773, 873,$ and 973 K. As clearly shown, the MD data can be very accurately described with linear regressions, with the coefficients of determination (R^2) for all systems and isotherms being higher than 0.996. Therefore, these linear fits can be safely used to extrapolate the diffusivity values at lower pressures. To this purpose, we consider $P = 1, 5, 10, 20,$ and 30 bar. For the extrapolated values of
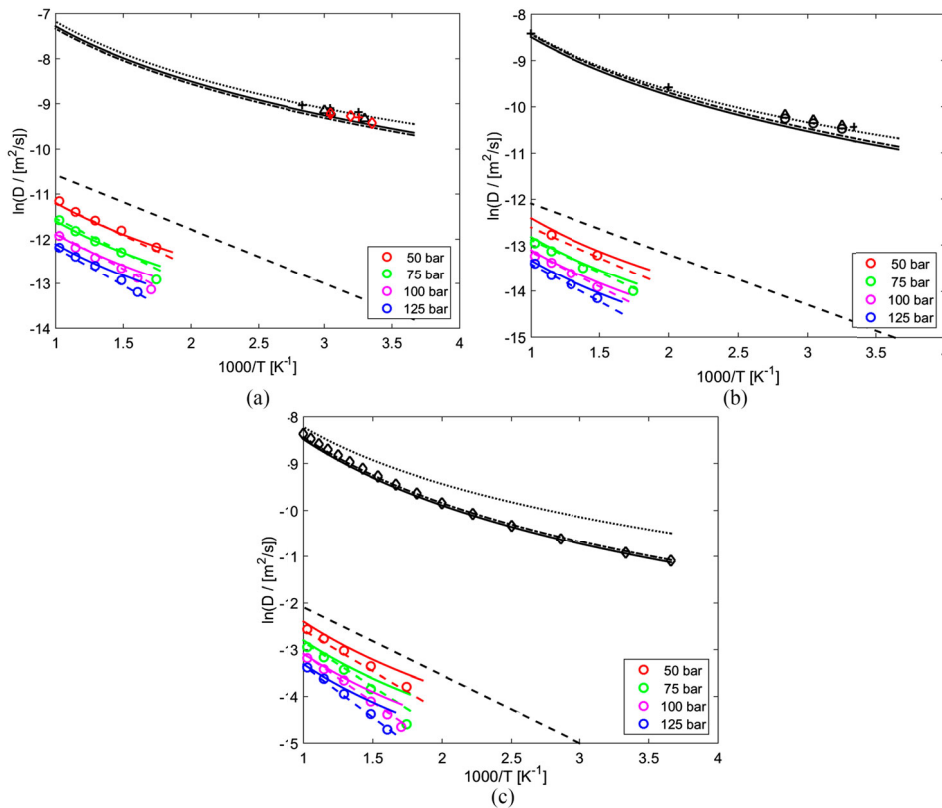
Figure 3. Comparison with experiments at 1 bar. Arrhenius-type plots of the computed/calculated intra-diffusion coefficients of H_2 in H_2O (a), O_2 in H_2O (b), pure H_2O accounting for water polarity (c), occurring in the vapour phase. Circles denote the MD simulations reported by Tsimpanogiannis et al. [10]. Dashed lines denote calculations with the correlation [Equation (8)]. Solid lines denote calculations with the CE theory. Lines of the black colour correspond to 1 bar. Dashed-dotted lines denote calculations with the Wilke and Lee [38] method, while dotted lines denote calculations with the Fuller et al. [40] method. Sources of experimental data: (a) Nelson [50] (red diamonds); Crider [51] (red crosses); Schwertz and Brow[52] (black crosses); McMurtie and Keyes [53] (black triangles), (b) Walker and Westenberg [54] (black crosses – measured values); Walker and Westenberg [54] (black triangles – extrapolated values); Schwertz and Brow[52] (black circles), and (c) Matsunaga and Nagashima [55] (black diamonds).
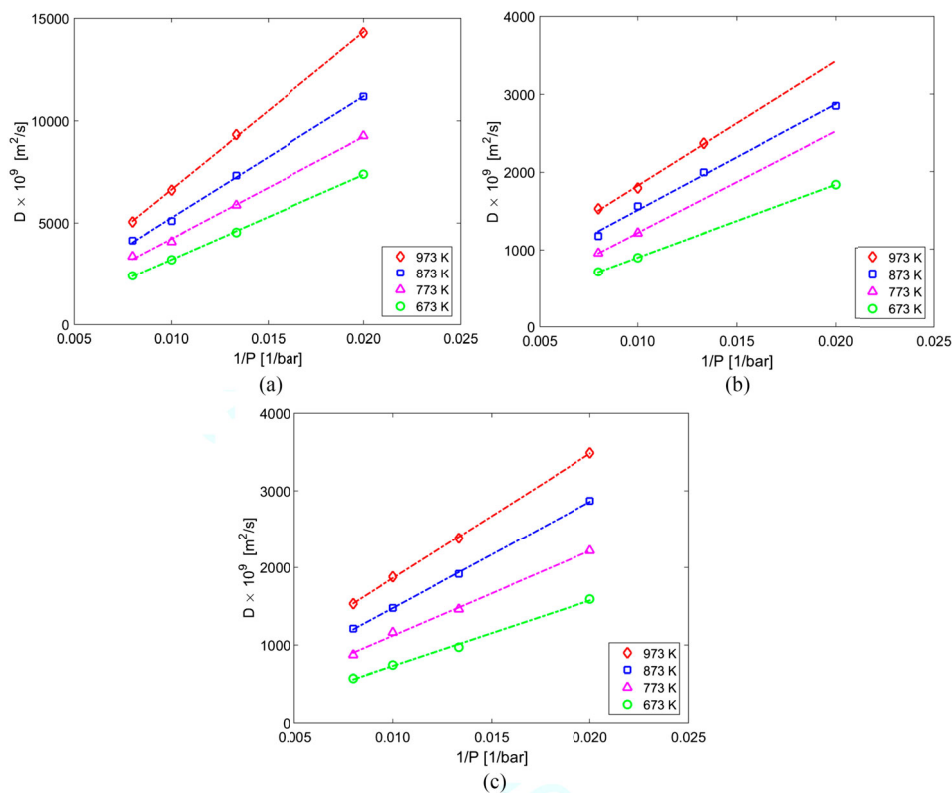
Figure 4. Intra-diddusion coefficients as a function of the inverse pressure (1/*P*) of H_2 in H_2O (a), O_2 in H_2O (b), pure H_2O accounting for water polarity (c), occurring in the vapour phase. Symbols denote the MD simulations reported by Tsimpanogiannis et al. [10] at four isotherms: 973.15 K (red diamonds), 873.15 K (blue squares), 773.15 K (magenta triangles), and 673.15 K (green circles). The dashed-dotted lines denote the current linear fits.
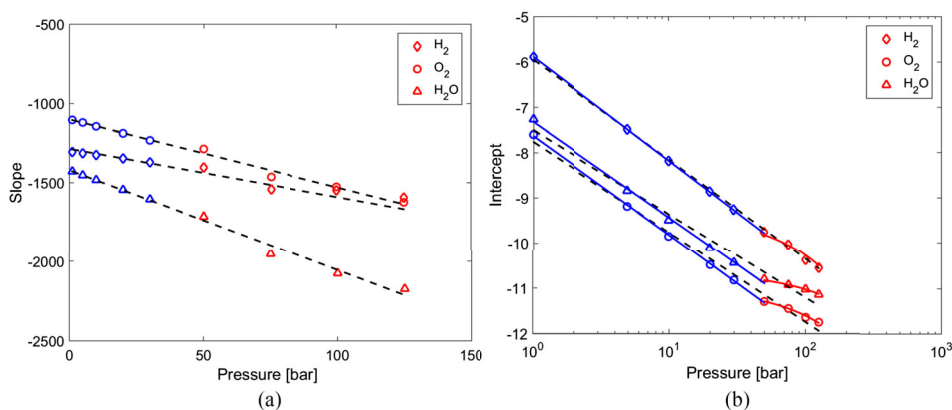
Figure 5. (a) Slopes and (b) intercepts of the fits to the diffusivity data for the H_2 in H_2O, O_2 in H_2O, and pure H_2O in the vapour phase. The red symbols denote the MD diffusivity data reported by Tsimpanogiannis et al. [10]. The blue symbols denote the extrapolated values calculated in the current study. The black dashed lines in (a) are fits using the parameters of Table 2. The black dashed lines in (b) are fits using the entire pressure range (1–125 bar). The blue solid lines in (b) are fits using the pressure range (1–50 bar) and the parameters provided in Table 2, while the red solid lines are the original fits [10] in the pressure range (50–125 bar) and the parameters provided in Table 1.

the diffusivities, we then follow a similar procedure to the one described in Tsimpanogiannis et al. [10]. Specifically, from an Arrhenius plot we obtain values for the intercept and the slope for each isobar. The calculated slopes and intercepts are shown in Figure 5(a,b) (denoted with blue symbols), respectively. The values computed with

MD simulations by Tsimpanogiannis et al. [10] at higher pressures (i.e. 50, 75, 100, and 125 bar), are also shown in Figure 5 (denoted with red symbols). As clearly evidenced in Figure 5(a), the calculated values for the slopes can still be correlated for the entire pressure range under consideration (i.e. 1–125 bar) with a linear function. The

Table 2. Parameters of the generalised Equation (9) for predicting the intra-diffusivities of infinitely diluted H_2 and O_2 in vapour H_2O, and the self-diffusivity of pure vapour H_2O in the current study.

	H_2 in H_2O	O_2 in H_2O	pure H_2O
m_0^*	$(-1.29 \pm 0.01) \times 10^3$	$(-1.10 \pm 0.01) \times 10^3$	$(-1.42 \pm 0.01) \times 10^3$
m_1^*	$(-0.31 \pm 0.02) \times 10^1$	$(-0.43 \pm 0.02) \times 10^1$	$(-0.63 \pm 0.02) \times 10^1$
n_0^*	-5.88 ± 0.04	-7.63 ± 0.03	-7.32 ± 0.01
n_1^*	-0.99 ± 0.03	-0.94 ± 0.03	-0.91 ± 0.01
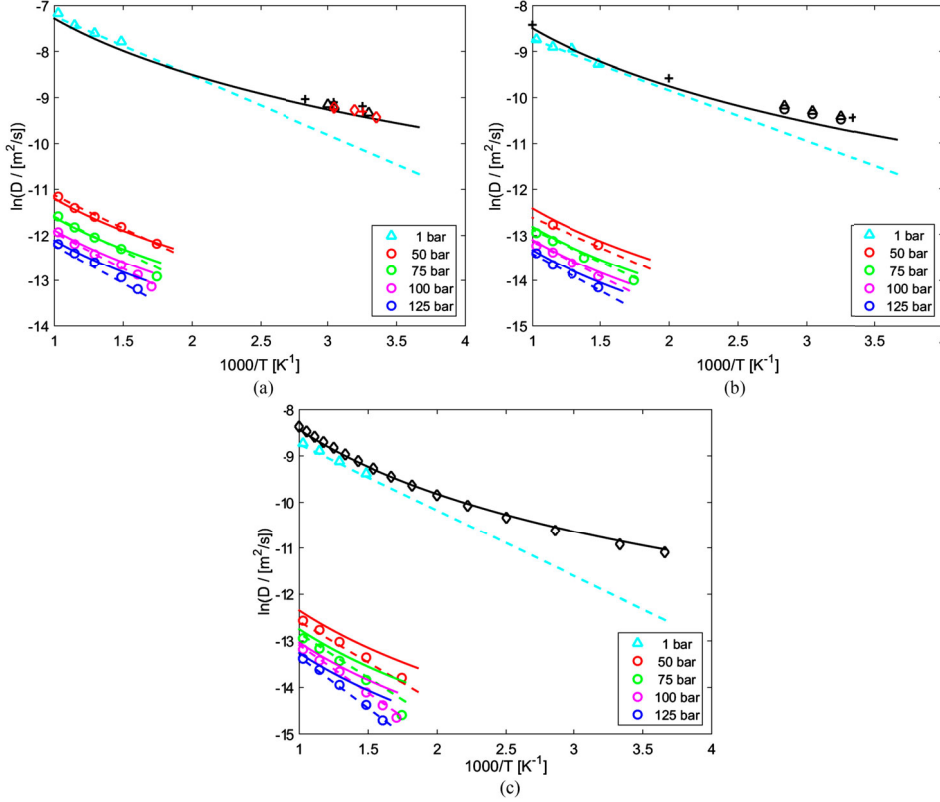
Figure 6. Comparison with experiments at 1 bar. Arrhenius-type plots of the computed/calculated intra-diffusion coefficients of H_2 in H_2O (a), O_2 in H_2O (b), pure H_2O accounting for water polarity (c), occurring in the vapour phase. Circles denote the MD simulations reported by Tsimpanogiannis et al. [10]. Dashed lines denote calculations with the correlation [Equation (8)]. Solid lines denote calculations with the CE theory. Turquoise triangles denote the current extrapolations of the MD simulations at 1 bar. Turquoise dashed line denotes calculations with the correlation [Equation (9)]. Lines of the black colour correspond to 1 bar. Sources of experimental data are the same as in Figure 3.

R^2 values of those fits equal 0.961, 0.991, and 0.991 for the H_2 and O_2 intra-diffusivities in vapour H_2O, and H_2O self-diffusion, respectively. Interestingly, the calculated intercepts for the entire pressure range cannot be correlated with a linear function as previously observed by Tsimpanogiannis et al. [10], but instead, a logarithmic function seems more appropriate. However, the quality of the fit of the calculated intercepts for the entire P range using a logarithmic function is not satisfactory, especially for the high P regime. This is clearly indicated in Figure 5(b) by the black dashed line. In sharp contrast, if only the pressures in the range of 1–50 bar are considered, the logarithmic fit is very accurate, with $R^2 =$ 1.000, 0.999, and 0.998 for H_2 and O_2 intra-diffusivities in vapour H_2O, and H_2O self-diffusivities, respectively.

Therefore, we recommend that at $P > 50$ bar, the correlation reported by Tsimpanogiannis et al. [10] should be used [Equation (8)], while at $P < 50$ bar, the following correlation should be used:

$$D = \exp\left[[n_1^* \ln(P) + n_0^*] + (m_1^* P + m_0^*) \, \frac{1}{T} \right] \quad (9)$$

where m_0^*, m_1^*, n_0^*, and n_1^* are fitting parameters. The values for these fitting parameters for the three systems considered here are listed in Table 2. The aforementioned behaviour can be further understood if we consider the Chapman and Enskog theory [see Equation (2)], where we observe that the pressure dependence of the diffusivity is $D \sim \frac{1}{P}$, therefore, $\ln(D) \sim \ln(P)$. On the other hand, the pressure dependence of the diffusivity in

Equation (8), reported in [10], is $\ln(D) \sim P$. This dependency was shown to be accurate for the narrow pressure range (50–125 bar) considered in [10], however it is not accurate for the wider pressure range (1–125 bar) considered here. Thus, the use of Equation (9) becomes essential.

Figure 6(a–c) show the comparison of the available experimental data with the MD projections at low pressures and the calculations with the new correlation [Equation (9)], for the H_2 and O_2 intra-diffusivities in vapour H_2O, and H_2O self-diffusivities, respectively. As can be observed, the extrapolated MD data (i.e. obtained from the linear fits, D vs. $1/P$) at 1 bar are in very good agreement with the calculations using the CE theory. Furthermore, very good agreement is observed between the extrapolated MD data, the new correlation [Equation (9)] and the available experimental data for the case of temperatures, $T > 400$ K, as can be seen in Figure 6(b ,c) for the cases of H_2 in H_2O and pure H_2O, respectively. Some deviations are observed at 1 bar between the CE theory and the new correlation [Equation (9)] for the lower temperatures (i.e. $T < 400$ K). This discrepancy may be due to the different functional for the temperature dependence between the CE theory and the correlation developed here.

4. Conclusions and future outlook

Significant effort has been devoted through the years in order to improve the calculations of intra- and self-diffusivities in binary and multi-component mixtures relevant to geological, chemical, biological, and environmental processes. The focus of the current study was diffusive processes with the solvent being in the vapour phase. To this purpose, available data from experiments and molecular simulations examining the intra-diffusivities of H_2 and O_2 in H_2O, and the self-diffusivity of pure H_2O (for pressure and temperature condition that the solvent is in the vapour phase) have been collected and subsequently compared against calculations based on the CE theory and the semi-empirical/semi-theoretical methods of (i) Wilke and Lee and (ii) Fuller et al. methods that are also based on the same theory. Comparisons between the MD simulations and the calculations using the CE theory or the semi-empirical methods in the pressure range 50–125 bar showed very good agreement. However, the extrapolation of the correlation [i.e. Equation (8)], reported in [10], to lower values and comparisons with experimental data at low pressures (1 bar) showed poor agreement. In order to rectify the aforementioned problem a novel methodology was proposed. in order to In particular, the molecular dynamics simulations performed at higher pressures (50–125 bar)

were extrapolated to lower pressures by observing the linear behaviour of the intra/self-diffusivities as function of the inverse pressure $(1/P)$ at low pressures. The extrapolated diffusivity values were subsequently used in order to further refine the original correlation [Equation (8)] and replace it with the currently recommended [Equation (9)], where a logarithmic dependency has been introduced in order to describe more accurately the behaviour.

It would be an interesting future outlook to explore the origins of the deviation between the MD simulations and the calculations from the CE theory at the proximity of the critical temperature. The performance of MD simulations at a more refined temperature grid (close to the critical point) may result in providing enough data points to replace the current linear dependency with a more refined one. In addition, performing new MD simulations at temperatures, $T > 973$ K, may shed light to the dependency of $\ln D$ vs. $1/T$. In that case, the agreement of Equation (9) with the CE theory could further improve. Finally, another interesting route to explore in a future study would be to consider mixtures with higher gas concentrations, in which the composition is expected to be an additional parameter in the predictive model for intra-diffusivities. For such systems, the mutual diffusivities (i.e. Maxwell-Stefan, Fickian) are also of interest since these diffusivities strongly depend on the composition of the mixture.

Disclosure statement

Funding

ORCID

Othonas A. Moultos http://orcid.org/0000-0001-7477-9684
Ioannis N. Tsimpanogiannis http://orcid.org/0000-0002-3466-1873

References

[1] M. Ball and M. Wietschel, Int. J. Hydrog. Energy **34** (2), 615–627 (2009). doi:10.1016/j.ijhydene.2008.11.014
[2] A. Ursua, L.M. Gandia and P. Sanchis, Proc. IEEE **100** (2), 410–426 (2012). doi:10.1109/JPROC.2011.2156750
[3] B. Jähne, G. Heinz and W. Dietrich, J. Geophys. Res. Oceans **92** (C10), 10767–10776 (1987). doi:10.1029/JC092iC10p10767
[4] I. Tsimpanogiannis, Y. Yortsos, S. Poulou, N. Kanellopoulos and A. Stubos, Phys. Rev. E. **59** (4), 4353–4365 (1999). doi:10.1103/PhysRevE.59.4353

[5] I.N. Tsimpanogiannis, Y.C. Yortsos and A.K. Stubos, Ind. Eng. Chem. Res. **39** (5), 1505–1513 (2000). doi:10.1021/ie9902434

[6] A. Yiotis, A. Boudouvis, A. Stubos, I. Tsimpanogiannis and Y. Yortsos, AIChE J. **50** (11), 2721–2737 (2004). doi:10.1002/(ISSN)1547-5905

[7] N. Heinemann, J. Alcalde, J.M. Miocic, S.J. Hangx, J. Kallmeyer, C. Ostertag-Henning, A. Hassanpoury-ouzband, E.M. Thaysen, G.J. Strobel, C. Schmidt-Hattenberger and K. Edlmann, Energy. Environ. Sci. **14** (2), 853–864 (2021). doi:10.1039/D0EE03536J

[8] B. Pan, X. Yin, Y. Ju and S. Iglauer, Adv. Colloid. Interface. Sci. **294**, 102473 (2021). doi:10.1016/j.cis.2021.102473

[9] I.N. Tsimpanogiannis, S.H. Jamali, I.G. Economou, T.J.H. Vlugt and O.A. Moultos, Mol. Phys. **118** (9-10), e1702729 (2020). doi:10.1080/00268976.2019.1702729

[10] I.N. Tsimpanogiannis, S. Maity, A.T. Celebi and O.A. Moultos, J. Chem. Eng. Data **66** (8), 3226–3244 (2021). doi:10.1021/acs.jced.1c00300

[11] I.N. Tsimpanogiannis and O.A. Moultos, Fluid. Phase. Equilib. **563**, 113568 (2022). doi:10.1016/j.fluid.2022.113568

[12] D.M. Himmelblau, Chem. Rev. **64** (5), 527–550 (1964). doi:10.1021/cr60231a002

[13] E.L. Cussler, *Diffusion: Mass Transfer in Fluid Systems*, 3rd ed. (Cambridge University Press, Cambridge, 2009).

[14] B.E. Poling, J.M. Prausnitz and J.P. O'Connel, *The Properties of Gases and Liquids*, 5th ed. (McGraw-Hill, Singapore, 2001).

[15] R.B. Bird, W.E. Stewart and E.N. Lightfoot, *Transport Phenomena*, 2nd ed. (John Wiley & Sons, New York, 2007).

[16] S. Chapman and T. Cowling, *The Mathematical Theory of Non-Uniform Gases*, (Cambridge University Press, Cambridge, 1970).

[17] A. Einstein, *Investigations on the Theory of Brownian Motion*, 1st ed. (Dover, New York, 1956).

[18] M.P. Allen and D.J. Tildesley, *Computer Simulation of Liquids*, 2nd ed. (Oxford University Press, Croydon, 2017).

[19] D. Frenkel and B. Smit, *Understanding Molecular Simulation: From Algorithms to Applications*, 2nd ed. (Elsevier, San Diego, California, 2001).

[20] R.S. Chatwell, G. Guevara-Carrion, Y. Gaponenko, V. Shevtsova and J. Vrabec, Phys. Chem. Chem. Phys. **23** (4), 3106–3115 (2021). doi:10.1039/D0CP04985A

[21] I.N. Tsimpanogiannis, O.A. Moultos, L.F. Franco, M.B.D.M. Spera, M. Erdős and I.G. Economou, Mol. Simul. **45** (4-5), 425–453 (2019). doi:10.1080/08927022.2018.1511903

[22] S. Kozlova, A. Mialdun, I. Ryzhkov, T. Janzen, J. Vrabec and V. Shevtsova, Phys. Chem. Chem. Phys. **21** (4), 2140–2152 (2019). doi:10.1039/C8CP06795C

[23] V.K. Michalis, O.A. Moultos, I.N. Tsimpanogiannis and I.G. Economou, Fluid Phase Equilib. **407**, 236–242 (2016). doi:10.1016/j.fluid.2015.05.050

[24] S. Páez, G. Guevara-Carrion, H. Hasse and J. Vrabec, Phys. Chem. Chem. Phys. **15** (11), 3985–4001 (2013). doi:10.1039/c3cp43785j

[25] X. Liu, A. Bardow and T.J.H. Vlugt, Ind. Eng. Chem. Res. **50** (8), 4776–4782 (2011). doi:10.1021/ie102515w

[26] X. Liu, S.K. Schnell, J.M. Simon, P. Krüger, D. Bedeaux, S. Kjelstrup, A. Bardow and T.J.H. Vlugt, Int. J. Thermophys. **34** (7), 1169–1196 (2013). doi:10.1007/s10765-013-1482-3

[27] O.A. Moultos, I.N. Tsimpanogiannis, A.Z. Panagiotopoulos and I.G. Economou, J. Chem. Thermodyn. **93**, 424–429 (2016). doi:10.1016/j.jct.2015.04.007

[28] O.A. Moultos, I.N. Tsimpanogiannis, A.Z. Panagiotopoulos and I.G. Economou, J. Phys. Chem. B **118** (20), 5532–5541 (2014). doi:10.1021/jp502380r

[29] O.A. Moultos, G.A. Orozco, I.N. Tsimpanogiannis, A.Z. Panagiotopoulos and I.G. Economou, Mol. Phys. **113** (17-18), 2805–2814 (2015). doi:10.1080/00268976.2015.1023224

[30] H.M. Polat, F. de Meyer, C. Houriez, C. Coquelet, O.A. Moultos and T.J. Vlugt, Fluid. Phase. Equilib. **564**, 113587 (2023). doi:10.1016/j.fluid.2022.113587

[31] P. Habibi, A. Rahbari, S. Blazquez, C. Vega, P. Dey, T.J.H. Vlugt and O.A. Moultos, J. Phys. Chem. B **126** (45), 9376–9387 (2022). doi:10.1021/acs.jpcb.2c06381

[32] N. Dawass, J. Langeveld, M. Ramdin, E. Pérez-Gallent, A.A. Villanueva, E.J.M. Giling, J. Langerak, L.J.P. van den Broeke, T.J.H. Vlugt and O.A. Moultos, J. Phys. Chem. B **126** (19), 3572–3584 (2022). doi:10.1021/acs.jpcb.2c01425

[33] W.A. van Rooijen, P. Habibi, K. Xu, P. Dey, T.J.H. Vlugt, H. Hajibeygi and O.A. Moultos, J. Chem. Eng. Data **In Press**, 2023. doi:10.1021/acs.jced.2c00707

[34] R.S. Brokaw, Ind. Eng. Chem. Proc. Des. Dev. **8** (2), 240–253 (1969). doi:10.1021/i260030a015

[35] J. Hirschfelder, C. Curtiss and R. Bird, *Molecular Theory of Gases and Liquids* (Wiley, New York, 1954).

[36] P.D. Neufeld, A. Janzen and R. Aziz, J. Chem. Phys. **57** (3), 1100–1102 (1972). doi:10.1063/1.1678363

[37] T.R. Marrero and E.A. Mason, J. Phys. Chem. Refer. Data **1** (1), 3–118 (1972). doi:10.1063/1.3253094

[38] C. Wilke and C. Lee, Ind. Eng. Chem. **47** (6), 1253–1257 (1955). doi:10.1021/ie50546a056

[39] E. Fuller and J. Giddings, J. Chromatogr. Sci. **3** (7), 222–227 (1965). doi:10.1093/chromsci/3.7.222

[40] E.N. Fuller, P.D. Schettler and J.C. Giddings, Ind. Eng. Chem. **58** (5), 18–27 (1966). doi:10.1021/ie50677a007

[41] E.N. Fuller, K. Ensley and J.C. Giddings, J. Phys. Chem. **73** (11), 3679–3685 (1969). doi:10.1021/j100845a020

[42] J.L.F. Abascal and C. Vega, J. Chem. Phys. **123** (23), 234505 (2005). doi:10.1063/1.2121687

[43] V. Buch, J. Chem. Phys. **100** (10), 7610–7629 (1994). doi:10.1063/1.466854

[44] M. Bohn, R. Lustig and J. Fischer, Fluid. Phase Equilib. **25** (3), 251–262 (1986). doi:10.1016/0378-3812(86)80001-2

[45] I.C. Yeh and G. Hummer, J. Phys. Chem. B **108** (40), 15873–15879 (2004). doi:10.1021/jp0477147

[46] O.A. Moultos, Y. Zhang, I.N. Tsimpanogiannis, I.G. Economou and E.J. Maginn, J. Chem. Phys. **145** (7), 074109 (2016). doi:10.1063/1.4960776

[47] S.H. Jamali, L. Wolff, T.M. Becker, A. Bardow, T.J.H. Vlugt and O.A. Moultos, J. Chem. Theory Comput. **14** (5), 2667–2677 (2018). doi:10.1021/acs.jctc.8b00170

[48] S.H. Jamali, A. Bardow, T.J.H. Vlugt and O.A. Moultos, J. Chem. Theory Comput. **16** (6), 3799–3806 (2020). doi:10.1021/acs.jctc.0c00268

[49] A.T. Celebi, S.H. Jamali, A. Bardow, T.J.H. Vlugt and O.A. Moultos, Mol. Simul. **47** (10-11), 831–845 (2021). doi:10.1080/08927022.2020.1810685

[50] E. Nelson, J. Appl. Chem. **6** (7), 286–292 (1956). doi:10.1002/jctb.5010060704

[51] W.L. Crider, J. Am. Chem. Soc. **78** (5), 924–925 (1956). doi:10.1021/ja01586a015

[52] F. Schwertz and J.E. Brow, J. Chem. Phys. **19** (5), 640–646 (1951). doi:10.1063/1.1748306

[53] R. McMurtrie and F. Keyes, J. Am. Chem. Soc. **70** (11), 3755–3758 (1948). doi:10.1021/ja01191a063

[54] R. Walker and A. Westenberg, J. Chem. Phys. **32** (2), 436–442 (1960). doi:10.1063/1.1730712

[55] N. Matsunaga and A. Nagashima, J. Phys. Chem. **87** (25), 5268–5279 (1983). doi:10.1021/j150643a042